Computational form-finding methods for fabric structures

by

Prof. W.J. Lewis Dip., Inz., MSc., PhD., CEng., MIStructE., FICE

School of Engineering, University of Warwick, Coventry CV4 7AL

Tel: 024 76 523 138; Fax: 024 76 418 922

Email: W.J.Lewis@warwick.ac.uk

Date: **21st June 2008**

Word count: **6111**

No. of Figures: **7**

No. of tables: **1**

Key words: ***Form-finding; fabric structures; design.***

A review of computational form-finding methods for fabric structures

Abstract

Form-finding is a process that determines the surface configuration of a fabric structure under pre-stress. This process can be carried out using a variety of numerical methods, of which the most common are: (i) transient stiffness, (ii) force density, and (iii) dynamic relaxation. This paper describes the three methods, discusses their advantages and limitations, and provides insights into their applicability as numerical tools for the design of fabric structures. Further, it describes various approaches to surface discretisation, and discusses consequences of using 'mesh control' and elastic effects in the design of form-found surfaces. A brief discussion of the general recommendations given in the European Design Guide for tensile surfaces structures concludes the paper.

1. Introduction

The design of a fabric structure differs from that used in conventional structural design in that it has to determine the shape of the canopy under prestress. The resulting surface geometry must satisfy the condition of static equilibrium and have as uniform stress distribution as possible. For these highly flexible structures, the process required to define their initial surface geometry is known as form-finding. As a concept, form-finding is not generally understood, except by specialists working in the area. Even then, the conviction that "I can build whatever shape I like" does arise occasionally. This problem stems from the fact that architects and engineers are used to dealing with structures of 'known' shape, i.e., rigid-type forms shaped at the outset by aesthetic and functional considerations. It is, therefore, difficult to come to terms with the fact that fabric structures are different; they adopt unique configurations under loading; configurations that, quite literally, have to be found.

Prior to 1970, form-finding of tension membrane structures was carried out using small-scale, physical models made of fabric or soap-film[1]. It was the design of the Munich Olympic complex in 1972 that marked the departure from the exclusive use of physical models in favour of computational form-finding and load analysis.

Currently, the three most commonly used computational form-finding methods, which have been implemented in commercial software, are known as:

(i) transient stiffness

(ii) force density

(iii) dynamic relaxation.

In all cases, regardless of the approach/method used, the process involves iterative computation aimed at producing a shape that is in static equilibrium.

Before discussing each of the methods in turn, it is worth noting that surface discretisation, i.e., the representation of the continuum by a system of inter-connected elements, is an important underlying factor influencing theoretical formulations and implementations of form-finding methods, as well as the accuracy of the solution.

The simplest surface discretisation is achieved using a mesh of line, or cable elements as shown in Fig. 1. In this case, the methodology adopted does not differ from that of the analysis of a tensioned cable net. This type of surface discretisation is used in each of the methods listed above, in order to explain their distinguishing features in a consistent and clear manner.

2. Transient stiffness method

The transient stiffness method[2,3] is based on small displacement theory that assumes linear dependence of deflections upon forces applied to the structure. The surface, discretised using line elements, forms a two-way system of cables intersecting at the nodes (Fig. 1).

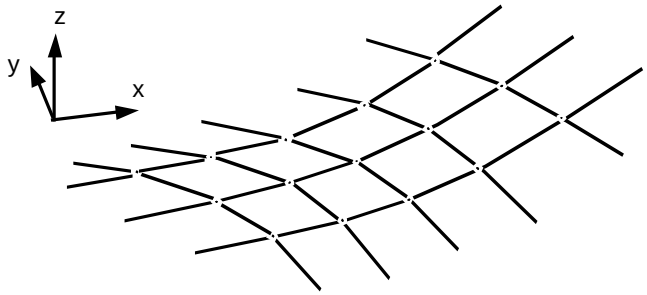

Fig. 1. Surface discretisation by line, or cable elements

The form-finding process starts with an assumed (guessed) surface configuration, $\{X\}$, between known boundaries, and an imposed tension field given by the initial pre-tension forces, T_m. Resolving T_m into global x, y, and z directions at the nodes

and summing up the contribution from each member sharing the same node, gives the resultant internal force vector, $\{\tilde{P}\}$.

As the system is unlikely to be in equilibrium, the resultant internal force $\{\tilde{P}\} \neq \{0\}$; it represents an out-of-balance, or residual force vector, $\{R\} = \{\tilde{P}\}$. Therefore, if $\{\delta\}$ is the vector of nodal displacements corresponding to the residual force vector,$\{R\}$, and $[K]$ is the global stiffness matrix, then it is possible to write:

$$[K]\{\delta\} = \{R\} \tag{1}$$

and determine the required displacements as:

$$\{\delta\} = [K]^{-1}\{R\} \tag{2}$$

However, there is a problem with the direct use of the above equation. Unless the initially guessed surface configuration is very close to the equilibrated, form-found surface, the residual force vector $\{R\}$ is likely to be large, and, therefore, the calculated vector of nodal displacements $\{\delta\}$ is also large. This invalidates the assumption of small displacements used in formulating [K]. Consequently, eqn.(2) can only be satisfied through an iterative process of calculating incremental residual forces and displacements, as explained below.

With k denoting the k^{th} iterative step, the current geometry of the structure is denoted by $\{X\}_k$, and the stiffness matrix calculated on the basis of this geometry is $[K]_k$. At k=0, the residual force vector $\{R\}_k$ can be calculated by resolving the internal forces at the nodes. In order to preserve the assumption of linear behaviour, a small proportion of this residual force vector, denoted as $\{\Delta R\}_k$ needs to be applied to find an increment in nodal displacement vector, $\{\Delta\delta\}$. Thus, at the next iterative step:

$$\{\Delta\delta\}_{k+1} = [K]_k^{-1}\{\Delta R\}_k \tag{3}$$

and a new geometry is:

$$\{X\}_{k+1} = \{X\}_k + \{\Delta\delta\}_{k+1} \tag{4}$$

The new geometry is used to calculate a new (updated) stiffness matrix, $[K]_{k+1}$. At this point, a new residual force vector, $\{R\}_{k+1}$ is found by resolving the forces again and a small proportion of it, $\{\Delta R\}_{k+1}$ is applied to find the next increment in the displacement vector, $\{\Delta\delta\}_{k+2}$ and the new (updated) geometry $\{X\}_{k+2}$.

The resulting iterative process of calculations continues until the residuals are reduced to (almost) zero, i.e. until the static equilibrium is reached. Experience is needed in selecting an appropriate value of $\{\Delta R\}_k$. Its magnitude should be small enough to ensure that the assumption of small displacements holds, and, at the same time, large enough the give a reasonable rate of convergence.

The numerical procedure presented above is known as the *'transient stiffness method*.' Accordingly, the stiffness matrix $[K]_k$ is referred to as a *transient stiffness matrix*, or *instantaneous stiffness matrix.* Although the numerical procedure is formulated in terms of the stiffness matrix changing with each iteration, it has been found that the convergence of the numerical solution is improved by keeping the stiffness matrix constant for a small number of consecutive steps.

2.1 Stiffness matrix

In form-finding, since we are not dealing with an actual material surface, elastic properties of the fabric can be ignored (see 2.1.1). Instead, a stiffness resulting from prestress, giving a change in the nodal forces consequent to a change in surface geometry, is used. This dependence is given by the geometric stiffness, [K^G]. Associated with it are the 'geometric' forces, as explained by the following example.

Figure 2 shows a member 1-2 displaced from state *'k'* to state *k*+1*'*. It can be seen that the incremental nodal displacement vector, $\{\Delta\delta_j\}$, may be replaced by a sum of vectors parallel and perpendicular (orthogonal) to the member in state *k*.

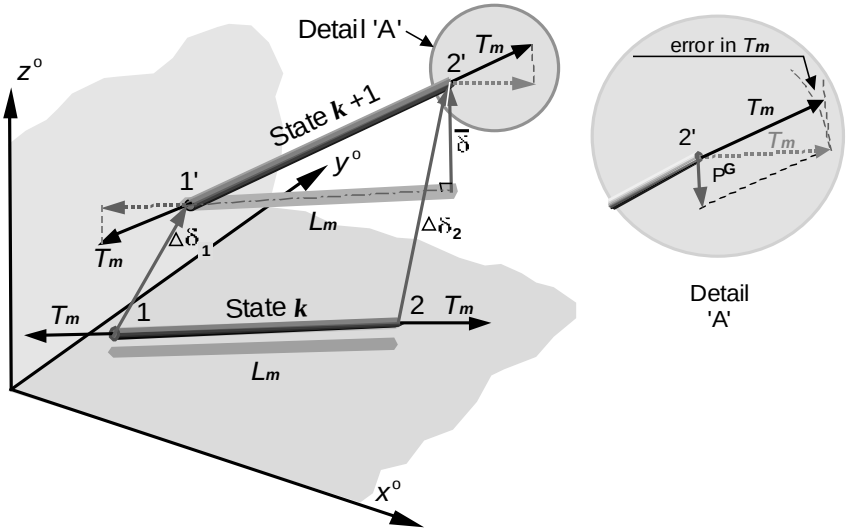

Fig. 2. Geometric forces in transient stiffness formulation

Hence

$$\{\Delta\delta_j\} = \{\Delta\delta_{j,\,par}\} + \{\Delta\delta_{j,\,orth}\} \qquad j = 1,\ 2 \tag{5}$$

The magnitude of the parallel vector $\{\Delta\delta_{j,par}\}$ is:

$$\left|\{\Delta\delta_{j,\,par}\}\right| = \{c\}^T\{\Delta\delta_j\} \tag{6}$$

where $\{c\}$ is the vector of direction cosines (Fig. 3), corresponding to the iterative state '*k*' .

The components of vector $\{\Delta\delta_{j,par}\}$ in global co-ordinates are:

$$\{\Delta\delta_{j,par}\} = \{c\}\{c\}^T\{\Delta\delta_j\}. \tag{7}$$

Now, the displacement vector orthogonal to the member is:

$$\{\Delta\delta_{j,orth}\} = \{\Delta\delta_j\} - \{c\}\{c\}^T\{\Delta\delta_j\} = \left[[I_3] - \{c\}\{c\}^T\right]\{\Delta\delta_j\}. \tag{8}$$

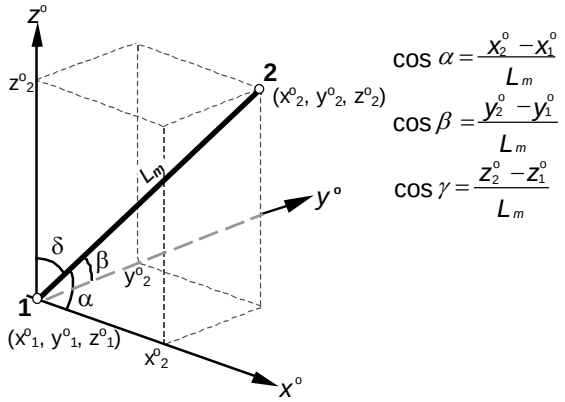

Fig. 3. Geometric illustration of direction cosines

It can be seen from Fig. 2 that for small angles of rotation, the difference between the orthogonal vectors of displacements at each end of the element can be taken as a measure of rotation, denoted by $\bar{\delta}$. Hence,

$$\left\{\bar{\delta}\right\} = \left\{\Delta\delta_{2,orth}\right\} - \left\{\Delta\delta_{1,orth}\right\} = \left[\left[I_3\right] - \left\{c\right\}\left\{c\right\}^T\right]\left\{\left\{\Delta\delta_2\right\} - \left\{\Delta\delta_1\right\}\right\} \tag{9}$$

The element carries the initial tension force, T_m. Provided the rotations are small, it can be assumed that the components of force T_m parallel to the element in state k+1 do not differ significantly from T_m. Hence the only 'new' components of forces are perpendicular ones. As the direction cosines enter the stiffness matrix formulation, and the calculation of stiffness lags one iteration behind, (eqn. (3)), these force components are perpendicular to the direction of the element in state k, not k+1. As a result, a degree of error is built into the formulation. The perpendicular force components of T_m are the 'geometric' forces, $\left\{P^G\right\}$, illustrated in Fig. 2.

For the system of nodal forces to be in equilibrium, the moment about end '1' generated by the initial tension force T_m on the lever arm $\left|\bar{\delta}\right|$ must be balanced by the moment due to the geometric force $\left\{P^G\right\}$ acting on the lever arm L_m. Thus, in scalar form,

$$P^G = T_m \frac{\bar{\delta}}{L_m} = K^G \bar{\delta}, \tag{10}$$

where $K^G = \frac{T_m}{L_m}$, given as the ratio of pre-stress force to the current length of member, is known as the geometric stiffness.

Substituting for $\bar{\delta}$ from eqn. (9) and using matrix notation, the geometric forces at each end of the element are:

$$\begin{aligned} \left\{P^G\right\} &= \frac{T_m}{L_m}\begin{Bmatrix} -\{\bar{\delta}\} \\ \{\bar{\delta}\} \end{Bmatrix} = \frac{T_m}{L_m}\begin{bmatrix} \left(I_3 - \{c\}\{c\}^T\right) & -\left(I_3 - \{c\}\{c\}^T\right) \\ -\left(I_3 - \{c\}\{c\}^T\right) & \left(I_3 - \{c\}\{c\}^T\right) \end{bmatrix} \left\{\Delta\delta_j\right\} \\ &= K^G \left\{\delta_j\right\}, \end{aligned} \tag{11}$$

The geometric stiffness defined in the above equation expresses a change in the nodal force components due to the presence of pre-stress when there is a change in the geometry of the structure during computation.

2.2 Evaluation of the method

2.2.1 The inclusion of elastic effects.

In some formulations [2,3,4,5] both the elastic and geometric effects are included in form-finding calculations. Such an approach is not, in principle, necessary, as form-finding calculations can apply to any type of material. Although the inclusion of the elastic stiffness matrix has the advantage of increasing of the overall stiffness, which helps to keep the increments of displacements $\left\{\Delta\delta_j\right\}$ small, at the same time, it introduces significant complications, such as:

- a need for control/monitoring of the values of the tension forces, which would vary significantly during the iterations, according to the elastic straining produced.

If not monitored, this situation could lead to a form-found configuration in which safe loads are exceeded

- a necessity for adjustments of the unstrained cable lengths, in order maintain the required tension levels (and prevent the problem stated above)
- a necessity for additional iterations, in order to restore static equilibrium after the adjustments to unstrained lengths of cables.

2.2.2 Accuracy

The transient stiffness method is critically dependent on the assumption of small displacements and rotations. Otherwise, large changes of geometry, which are common in the initial stages of computational form-finding, would result in the nodal forces and nodal displacements not being related to each other correctly. Potentially, this could lead to either a lack of convergence of the solution, or a wrong solution.

The transient stiffness matrix requires numerous matrix manipulations, even for small systems. For large systems, if matrix inversion is used, the solution may be prone to divergence, or yield useless results, due to computational round-off errors, exacerbated by ill-conditioning. A matrix is said to be ill-conditioned, if it contains coefficients that are orders of magnitude greater (or smaller) than other coefficients. The problems likely to arise in arithmetic operations on of ill-conditioned matrices include 'swamping' the effects of small terms, or 'loss of significance' in the case of small differences between large numbers containing too few figures to maintain accuracy [6].

To mitigate round-off, techniques such as scaling of the stiffness matrix[6,7] are recommended, but they add to the computational effort. It is well-known [7, 8] that if the size of the matrix is n x n, then the total number of arithmetic operations required for matrix inversion (and hence the computing time) is proportional to n^3.

3. Force density

The force density method [9,10] was developed simultaneously with the transient stiffness to facilitate the design of the Munich Olympic roofs. The method uses a surface discretised as a system of branches. A simple branch of just four cables is shown in Fig. 4. Nodes 2 to 5 represent boundary points with known co-ordinates, expressed in the global x^o, y^o and z^o system.

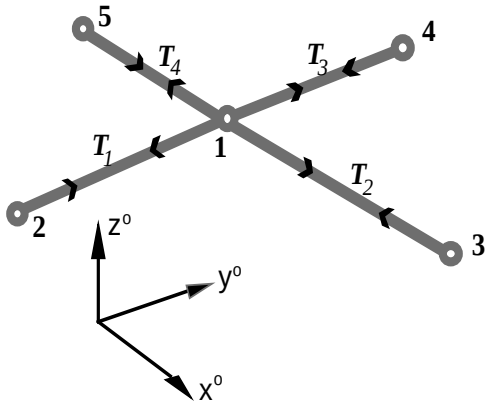

Fig. 4. A branch of elements

The equations of equilibrium of forces at node 1 are obtained by resolving the tension forces T_1 - T_4 into the global components, and summing up their respective contributions at the common node. Hence:

$$\begin{aligned}
&\frac{T_1\left(x_2^o - x_1^o\right)}{L_1} + \frac{T_2\left(x_3^o - x_1^o\right)}{L_2} + \frac{T_3\left(x_4^o - x_1^o\right)}{L_3} + \frac{T_4\left(x_5^o - x_1^o\right)}{L_4} = \tilde{P}_{x^o} = 0 \\
&\frac{T_1\left(y_2^o - y_1^o\right)}{L_1} + \frac{T_2\left(y_3^o - y_1^o\right)}{L_2} + \frac{T_3\left(y_4^o - y_1^o\right)}{L_3} + \frac{T_4\left(y_5^o - y_1^o\right)}{L_4} = \tilde{P}_{y^o} = 0 \qquad (12) \\
&\frac{T_1\left(x_2^o - x_1^o\right)}{L_1} + \frac{T_2\left(x_3^o - x_1^o\right)}{L_2} + \frac{T_3\left(x_4^o - x_1^o\right)}{L_3} + \frac{T_4\left(x_5^o - x_1^o\right)}{L_4} = \tilde{P}_{x^o} = 0
\end{aligned}$$

In the above system of equations, the member lengths L_m, (m = 1,...4) are non-linear functions of the co-ordinates of points (nodes) that define the members. Both are

unknown. By introducing constant values of tension coefficients, or **force densities,** q_m, defined as a ratio of member force to member length, viz., $q_m = \frac{T_m}{L_m}$, the system of equations becomes linear, viz.,

$$\begin{aligned} q_1\left(x_2^{\mathrm{o}} - x_1^{\mathrm{o}}\right) + q_2\left(x_3^{\mathrm{o}} - x_1^{\mathrm{o}}\right) + q_3\left(x_4^{\mathrm{o}} - x_1^{\mathrm{o}}\right) + q_4\left(x_5^{\mathrm{o}} - x_1^{\mathrm{o}}\right) = 0 \\ q_1\left(y_2^{\mathrm{o}} - y_1^{\mathrm{o}}\right) + q_2\left(y_3^{\mathrm{o}} - y_1^{\mathrm{o}}\right) + q_3\left(y_4^{\mathrm{o}} - y_1^{\mathrm{o}}\right) + q_4\left(y_5^{\mathrm{o}} - y_1^{\mathrm{o}}\right) = 0 \\ q_1\left(z_2^{\mathrm{o}} - z_1^{\mathrm{o}}\right) + q_2\left(z_3^{\mathrm{o}} - z_1^{\mathrm{o}}\right) + q_3\left(z_4^{\mathrm{o}} - z_1^{\mathrm{o}}\right) + q_4\left(z_5^{\mathrm{o}} - z_1^{\mathrm{o}}\right) = 0 \end{aligned} \tag{13}$$

With the q_{m} values known, the co-ordinates of node 1 can now be found, as:

$$x_1^{\mathrm{o}} = \frac{q_1 x_2^{\mathrm{o}} + q_2 x_3^{\mathrm{o}} + q_3 x_4^{\mathrm{o}} + q_4 x_5^{\mathrm{o}}}{q_1 + q_2 + q_3 + q_4} \tag{14}$$

and similarly for the y_1^{o}, and z_1^{o} directions.

3.1 Matrix formulation

In a general case, for a member m with end nodes j and n, the length components L_{mx}, L_{my}, and L_{mz} of the vector $\{L_m\}$ can be expressed using connectivity matrix [C] and their nodal co-ordinates as in:

$$\begin{aligned} L_{mx} &= x_j^{\mathrm{o}} - x_n^{\mathrm{o}} = \begin{bmatrix} 1 & -1 \end{bmatrix} \begin{Bmatrix} x_j^{\mathrm{o}} \\ x_n^{\mathrm{o}} \end{Bmatrix} = [C]\{X\} \\ L_{my} &= y_j^{\mathrm{o}} - y_n^{\mathrm{o}} = \begin{bmatrix} 1 & -1 \end{bmatrix} \begin{Bmatrix} y_j^{\mathrm{o}} \\ y_n^{\mathrm{o}} \end{Bmatrix} = [C]\{Y\} \\ L_{mz} &= z_j^{\mathrm{o}} - z_n^{\mathrm{o}} = \begin{bmatrix} 1 & -1 \end{bmatrix} \begin{Bmatrix} z_j^{\mathrm{o}} \\ z_n^{\mathrm{o}} \end{Bmatrix} = [C]\{Z\} \end{aligned} \tag{15}$$

In the case of the structure shown in Fig. 4, the projected lengths of members 1 to 4 in the x- direction can be expressed as:

$$\begin{Bmatrix} L_{1x} \\ L_{2x} \\ L_{3x} \\ L_{4x} \end{Bmatrix} = \underbrace{\begin{bmatrix} -1 & 1 & 0 & 0 & 0 \\ -1 & 0 & 1 & 0 & 0 \\ -1 & 0 & 0 & 1 & 0 \\ -1 & 0 & 0 & 0 & 1 \end{bmatrix}}_{[C]} \begin{Bmatrix} x_1^o \\ x_2^o \\ x_3^o \\ x_4^o \\ x_5^o \end{Bmatrix}}_{\{X\}} = \begin{Bmatrix} x_2^o - x_1^o \\ x_3^o - x_1^o \\ x_4^o - x_1^o \\ x_5^o - x_1^o \end{Bmatrix}, \tag{16}$$

where [C] is the connectivity matrix. In order to prevent the matrix becoming sparse, and to facilitate computations, the following convention has been found helpful: number the internal nodes first, and the boundary ones last.

Extending to *y* and *z* directions, the general form is

$$\begin{aligned} \{L_{mx}\} &= [C]\{X\} \\ \{L_{my}\} &= [C]\{Y\} \\ \{L_{mz}\} &= [C]\{Z\} \end{aligned} \tag{17}$$

The *x*, *y* and *z* components of internal forces in cable members, given by, $\tilde{P}_{mx}$, $\tilde{P}_{my}, \tilde{P}_{mz}$, respectively can be expressed as a product of force densities, q_m, and projected member lengths, which, in matrix notation, are:

$$\begin{aligned} [\tilde{P}_{mx}] &= [Q]\{L_{mx}\} \\ [\tilde{P}_{my}] &= [Q]\{L_{my}\} \\ [\tilde{P}_{mz}] &= [Q]\{L_{mz}\} \end{aligned} \quad , \tag{18}$$

where [*Q*] is the diagonal matrix of force densities,

$$[Q] = \begin{bmatrix} q_1 & \cdot & \cdot & \cdot \\ \cdot & q_2 & \cdot & \cdot \\ \cdot & \cdot & q_3 & \cdot \\ \cdot & \cdot & \cdot & q_4 \end{bmatrix} \tag{19}$$

At each node of the structure, the sum of the *x*, *y* and *z* components of the internal forces $\tilde{P}_m$ in members connecting to the given node must balance the external load vector $\{P\}$ applied to these nodes. Hence:

$$\begin{aligned} \sum \tilde{P}_{mx} &= P_{x^{\mathrm{o}}} \\ \sum \tilde{P}_{my} &= P_{y^{\mathrm{o}}} \\ \sum \tilde{P}_{mz} &= P_{z^{\mathrm{o}}} \end{aligned} \tag{20}$$

Substituting for $\tilde{P}_{mx}$, $\tilde{P}_{my}$, $\tilde{P}_{mz}$ from eqns. (18) and (17), and noting that the summation in eqn. (20) can be carried out by pre-multiplying the internal force components $\tilde{P}_{mx}$, $\tilde{P}_{my}$, and $\tilde{P}_{mz}$ by $[C]^T$, leads to the matrix form :

$$\begin{aligned} [C]^T[Q][C]\{X\} &= \{P_{x^{\mathrm{o}}}\} \\ [C]^T[Q][C]\{Y\} &= \{P_{y^{\mathrm{o}}}\} \\ [C]^T[Q][C]\{Z\} &= \{P_{z^{\mathrm{o}}}\} \end{aligned} \tag{21}$$

Applying this result to the five-node, four-member structure shown in Fig. 4, gives, for the *x* direction:

$$[C]^{\mathrm{T}}[Q][C]\{X\} = \begin{bmatrix} -1 & -1 & -1 & -1 \\ 1 & 0 & 0 & 0 \\ 0 & 1 & 0 & 0 \\ 0 & 0 & 1 & 0 \\ 0 & 0 & 0 & 1 \end{bmatrix} \begin{bmatrix} q_1 & \cdot & \cdot & \cdot \\ \cdot & q_2 & \cdot & \cdot \\ \cdot & \cdot & q_3 & \cdot \\ \cdot & \cdot & \cdot & q_4 \end{bmatrix} \begin{Bmatrix} x_2^{\mathrm{o}} - x_1^{\mathrm{o}} \\ x_3^{\mathrm{o}} - x_1^{\mathrm{o}} \\ x_4^{\mathrm{o}} - x_1^{\mathrm{o}} \\ x_5^{\mathrm{o}} - x_1^{\mathrm{o}} \end{Bmatrix} = \begin{Bmatrix} P_{1x^{\mathrm{o}}} \\ P_{2x^{\mathrm{o}}} \\ P_{3x^{\mathrm{o}}} \\ P_{4x^{\mathrm{o}}} \\ P_{5x^{\mathrm{o}}} \end{Bmatrix} \tag{22}$$

In the above system of equations, P_{1x^o} is zero and the remaining forces are equal to the x-components of the reactions at the boundaries (nodes 2-5). Hence:

$$[C]^T[Q][C]\{X\} = \begin{bmatrix} -q_1 & -q_2 & -q_3 & -q_4 \\ q_1 & 0 & 0 & 0 \\ 0 & q_2 & 0 & 0 \\ 0 & 0 & q_3 & 0 \\ 0 & 0 & 0 & q_4 \end{bmatrix} \begin{Bmatrix} x_2^o - x_1^o \\ x_3^o - x_1^o \\ x_4^o - x_1^o \\ x_5^o - x_1^o \end{Bmatrix} = \begin{Bmatrix} 0 \\ P_{2x^o} \\ P_{3x^o} \\ P_{4x^o} \\ P_{5x^o} \end{Bmatrix} \qquad (23)$$

The equilibrium equations in the remaining *y* and *z* directions can be expanded in the similar manner.

From eqn. (23) the *x*-co-ordinate of node 1 is:

$$x_1^o = \frac{q_1 x_2^o + q_2 x_3^o + q_3 x_4^o + q_4 x_5^o}{q_1 + q_2 + q_3 + q_4} ,$$

(confirming the earlier result), and the remaining external force components are given as:

$$q_1\left(x_2^o - x_1^o\right) = P_{2x^o}; \quad q_2\left(x_3^o - x_1^o\right) = P_{3x^o}; \quad q_3\left(x_4^o - x_1^o\right) = P_{4x^o}; \quad q_4\left(x_5^o - x_1^o\right) = P_{5x^o} \qquad (24)$$

3.2 Evaluation of the method

With boundary configurations known or assumed, the only other factor controlling the shape of the structure is the value of force densities. This, theoretically, provides an opportunity for generating an infinite number of network configurations. However, such configurations may compromise the uniformity of the tension field i.e., they may carry unacceptably high range of tension forces. It is clear that a constant value of force density will not, in general, produce constant tensions, unless the calculated lengths of the elements happen to be constant. From the practical point of view, the results should produce a network with, 'more or less', equal forces in them, so that none of the elements would get over-stressed when imposed loads are applied (at the

load analysis stage). It has been found that a value of force density quoted as producing reasonable results is 1 for all inner cables, and a value inversely proportional to the cable length for boundary cables, when such cables have irregular lengths [11,12].

In general, the system of linear equations given by the force density approach cannot be solved directly, because of the size of the matrix. The limitations of the force density method were realised quite early, and this has led to further developments, to include additional constraints, such as the preservation of rectangular, or equidistant meshes[11.] More recent additions include the facility to model minimal surface forms by preserving a constant tension field[13]. In such cases, the formulation becomes a non-linear force density method and requires additional iterative procedures to satisfy the required condition. Some researchers[14] advocate the use of surface minimisation through least squares fit to arrive at a minimal surface solution. In the opinion of the author, surface minimisation is not a robust criterion for convergence of the solution[15]; it would require a very fine mesh of elements and the sum of their area would be subject of a cumulative round off error.

4. Dynamic relaxation method

Unlike the previous two methods, dynamic relaxation does not rely on the global stiffness matrix formulation for the solution of the system of non-linear equilibrium equations. The algorithm uses a 'lumped mass' model, in which the mass of a discretised continuum is assumed to be concentrated (lumped) at the nodes of the surface. In the iterative scheme, the out-of-balance forces are relaxed, at each node in turn, until they are close to zero. The solution follows a process in which static equilibrium of the system is achieved by simulating a pseudo-dynamic process in

time'. In essence, under the influence of loading (out-of-balance internal forces), a system of lumped masses oscillates about the equilibrium position and eventually comes to rest under the influence of damping. In its original form, the method makes use of viscous damping, as described in the following section.

4.1 Dynamic relaxation method with viscous damping

The method is based on the equation of motion, which, for a discretised system is given by:

$$P_{ji} = \left[\sum K\delta\right]_{ji} + M_{ji}\ddot{\delta}_{ji} + C\dot{\delta}_{ji} \qquad (25)$$

where

subscript *ji* refers to the j^{th} node in the i^{th} direction in a discretised system,

P_{ji} is the vector of external loads,

$\left[\sum K\delta\right]_{ji}$ is the vector of internal loads, (with K representing nodal stiffness and δ displacements and the summation applying to the connected nodes only),

$\ddot{\delta}_{ji}, \dot{\delta}_{ji}$, are the vectors of nodal accelerations and velocities, respectively,

C is the coefficient of viscous damping

M_{ji} is the mass lumped to the nodes .

Introducing the nodal residual forces, R_{ji} as the difference between the external and internal force vectors, gives

$$R_{ji} = P_{ji} - \left[\sum K\delta\right]_{ji} \qquad (26)$$

The above equation applies to the load analysis, which follows the form finding stage and which includes elastic straining components in the formulated stiffness matrix, [K]. In form-finding, it is preferable not include elastic effects and since there is no

external load acting on the inner nodes of the structure (whose configuration we are trying to find), the residual forces are simply equal to the internal force vector, $\tilde{P}_{ji}$.

Hence,

$$R_{ji} = \tilde{P}_{ji} \tag{27}$$

$\tilde{P}_{ji}$ is found from the resolution of the internal forces, T_m, at the nodes of the structure.

Also, from eqn. (26)

$$M_{ji}\ddot{\delta}_{ji} + C\dot{\delta}_{ji} = R_{ji}\cdot \tag{28}$$

Equation (28) states that the motion of a system is produced by the out-of-balance forces. The condition of static equilibrium requires these forces to come to zero.

Equation (28) is approximated by centred finite differences in which the acceleration term is represented by the variation of velocities over the time interval, Δt, and the velocity term as an average over the same interval. Thus, with k denoting the time interval at which variables are calculated, the residual forces at time increment $k\Delta t$ are given by:

$$R_{ji}^{k} = M_{ji}\frac{\dot{\delta}_{ji}^{k+\frac{1}{2}} - \dot{\delta}_{ji}^{k-\frac{1}{2}}}{\Delta t} + C\frac{\dot{\delta}_{ji}^{k+\frac{1}{2}} + \dot{\delta}_{ji}^{k-\frac{1}{2}}}{2}, \tag{29}$$

which gives the recurrence equation for velocities:

$$\dot{\delta}_{ji}^{k+\frac{1}{2}} = \left\{\dot{\delta}_{ji}^{k-\frac{1}{2}}\frac{\frac{M_{ji}}{\Delta t} - \frac{C}{2}}{\frac{M_{ji}}{\Delta t} + \frac{C}{2}}\right\} + \frac{R_{ji}^{k}}{\frac{M_{ji}}{\Delta t} + \frac{C}{2}} \quad . \tag{30}$$

The velocities are then used to predict displacements at time k+1:

$$\delta_{ji}^{k+1} = \delta_{ji}^{k} + \dot{\delta}_{ji}^{k+\frac{1}{2}}\Delta t\cdot \tag{31}$$

The iterative process of arriving at static equilibrium consists of a repetitive use of eqns. (30) and (31) until the residual forces are close to zero.

4.1.1 Stability and convergence of the iterative solution

The criterion for assured convergence [15,16,17], is given by

$$\Delta t_{\max} = \sqrt{2\frac{M}{K}} \tag{32}$$

The time increment Δt=1 is both convenient and the one that satisfies the limit for stability of the numerical solution. Thus, for Δt=1, the mass at any node should be set to comply with eqn.(32), viz.,

$$M_{ji} = \frac{\Delta t^2 K_{ji}}{2} = \frac{K_{ji}}{2} \tag{33}$$

4.1.2 Critical viscous damping coefficient

In an un-damped mode, the structure will oscillate about its position of equilibrium. If N denotes the number of iterations required to complete one cycle of oscillations in a fundamental mode, then the viscous damping coefficient, known as critical damping, can be found from[15]:

$C=4\pi mf$, (34)

where $f=1/N\Delta t$, is the fundamental frequency of oscillations.

In order to obtain N, an additional computer run is necessary, with C set to zero. The resulting un-damped oscillations of the structure are then used to calculate the value of the critical viscous damping coefficient from eqn. (34).

Critical damping, which is based on the lowest natural frequency of the system, gives the fastest convergence. If the damping coefficient is below this value, (the structure is said to be 'under-damped') the solution may overshoot the static equilibrium of the system, before settling down to convergence. This situation is preferred to the case of an 'over-damped' solution, in which the convergence may proceed at a very slow pace.

The requirement for a two-stage solution procedure is rather inconvenient. For this reason, the method has been superseded by the dynamic relaxation technique with *kinetic damping*.

4.2 Dynamic Relaxation method with kinetic damping

4.2.1 General

When the technique of kinetic damping is employed, the viscous damping coefficient is taken as zero and the system of oscillating masses is brought to rest by following a process of stopping the iterations whenever a peak in kinetic energy of the entire system is detected. The computation is then re-started from the current configuration, but with zero initial velocity[15, 16]. This process relies on the observation that, in simple harmonic motion, maximum kinetic energy is achieved in a configuration that corresponds to a minimum potential energy. A simple illustration of that is a motion of a pendulum, which, once set in motion, eventually comes to rest in its position of minimum potential energy. In the dynamic relaxation algorithm, the movement of the structure is mapped by the successive iterations. The pendulum analogy shows that stopping that movement (iterations) at the points of maximum kinetic energy is equivalent to achieving a stable equilibrium position. However, because the frequency of the oscillations of individual nodes varies, it is not possible to achieve

true overall equilibrium of the structure after the first kinetic energy peak. During the next iterations, the velocities and the displacements accumulate, but in increments decreasing in magnitude, as the residual forces become smaller with each iterative step. This results in the peaks of kinetic energy gradually becoming less pronounced, and eventually the whole system settling down to static equilibrium. The formulation of the dynamic relaxation algorithm with kinetic damping is described below.

With the viscous damping coefficient equal to zero, and the time increment Δt=1, equation (30) in centred finite difference form[6], is:

$$R_{ji}^{k} = M_{ji}\left(\dot{\delta}_{ji}^{k+\frac{1}{2}} - \dot{\delta}_{ji}^{k-\frac{1}{2}} \right). \tag{35}$$

Implementing the numerical stability criterion given by eqn. (33) gives

$$R_{ji}^{k} = \frac{K_{ji}}{2}\left(\dot{\delta}_{ji}^{k+\frac{1}{2}} - \dot{\delta}_{ji}^{k-\frac{1}{2}} \right)$$

Consequently, the recurrence equations for velocities and displacements are:

$$\dot{\delta}_{ji}^{k+\frac{1}{2}} = \left\{ \dot{\delta}_{ji}^{k-\frac{1}{2}} \right\} + \frac{R_{ji}^{k}}{\frac{1}{2}K_{ji}}. \tag{36}$$

and

$$\delta_{ji}^{k+1} = \delta_{ji}^{k} + \dot{\delta}_{ji}^{k+\frac{1}{2}} \cdot 1. \tag{37}$$

As can be seen form the above, the method makes use of the nodal stiffness, K_{ji}. The stiffness needed here is the geometric stiffness, lumped at the nodes, viz.,

$$K_{ji}^{G} = \sum K_{m}^{G}$$

where K_{m}^{G} is the geometric stiffness of elements '*m*' connecting to a given node, defined in eqn (10).

4.2.2 Iterative process

Equations (27), (36) and (37) form an iterative loop of the dynamic relaxation algorithm with kinetic damping. At kinetic energy peak, velocities are set to zero and the whole system is re-started from the current configuration. It can be deduced that kinetic energy peak has occurred when the latest value of the kinetic energy is noted to be smaller than that in the previous iteration. With the iterative process punctuated by discrete time intervals, Δt, the precise location of the point at which a maximum value of kinetic energy has occurred is not known, but can be estimated. It is important to do so, in order to correct the displacements, as these would have been calculated after a kinetic energy peak has occurred. The point of maximum kinetic energy can be found by assuming that the trace of the kinetic energy curve represents a quadratic variation with the number of iterations. If the time at which the kinetic energy peak has occurred is denoted by $t^{\max}$, and KE_1, KE_2, and KE_3, denote three sequential energy levels at some point during iterations in which $KE_3 < KE_2$, it can be shown that[15]

$$t^{\max} = -\frac{4KE_2 - 3KE_1 - KE_3}{KE_3 - 2KE_2 + KE_1}, \tag{38}$$

and the corrected displacements at t^{max} are:

$$\delta_{ji}^{(k+1)-corr} = \delta_{ji}^{(k+1)} - (1+\beta)\dot{\delta}_{ji}^{(k-\frac{1}{2})} - \frac{2R_{ji}^{k}}{K_{ji}} \quad , \tag{39}$$

where

$$\beta = \frac{KE_3 - KE_2}{KE_3 - 2KE_2 + KE_1}. \tag{40}$$

When kinetic energy peak is detected, the displacements are calculated according to eqn.(39), but otherwise, eqn. (37) is used.

4.3 Evaluation of the method

The main advantage of the method is the small number of arithmetic operations that need to be carried out at any one time, since the computations are concerned with one node in turn, rather than all nodes simultaneously. Such an approach minimises computational round-off errors, and contributes to stability and accuracy of the numerical solution. It has been shown[15,18] that the method is more efficient than the transient stiffness solution.

Experience has shown[15,16] that the numerical stability criterion for the dynamic relaxation method is robust, provided the largest direct stiffness of the connecting elements is used to ensure as small as possible size of the iterative step. The criterion is based on the assumption of constant mass and stiffness. A derivation of a stability criterion based on variable lumped mass and stiffness would be an advantage, and this subject merits further study. The method is stable and capable of providing solutions to highly non-linear problems, even if the criteria of constant mass and stiffness are not met. However, to ensure fast convergence and stability of iterations, it is recommended that the difference in nodal stiffness throughout the structure is kept small. This can be achieved by an appropriate surface discretisation, involving the same, or similar, number of elements connecting to each node of the structure.

4.4 Surface discretisation and accuracy of modelling

4.4.1 Line elements

Surface discretisation by means of line elements is equivalent to replacing the surface by a cable net. Such a net, when used to model stable minimal surfaces (soap-films) has all its elements in constant tension and the elements following geodesic paths[15]. For relatively shallow surfaces, the results are reasonably accurate, but for surfaces

with more pronounced curvatures, the cables have a tendency to cluster in the areas of high curvature and become sparse elsewhere. This phenomenon is illustrated in Fig. 5, which shows a saddle shaped surface modelled with cable elements of constant tension.

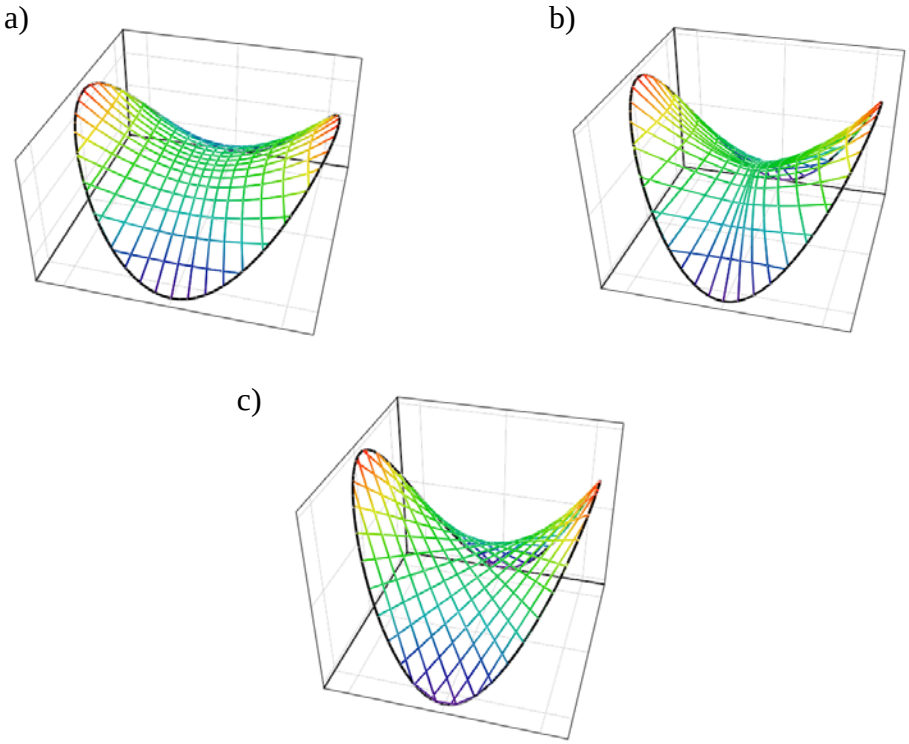

Fig. 5. Line element representation of a saddle-shaped surface modelled by constant tension cables

There are 15 cables in each direction and the boundary of the structure projects as a circle of 6 unit's radius. The aspect ratio of height to radius is 0.528 for case (a) and 0.846 for cases (b) and (c). It can be seen that with the rising aspect ratio, the cables start to cluster in the area of high curvature (case (b)). Improvements in the final surface definition can be made by carefully selecting the location of the end points, so that after form-finding the cables slip into their equilibrium position while maintaining a reasonably uniform spacing. This is illustrated in case (c).

4.4.2 Triangular elements

The most common type of surface element used in conjunction with dynamic relaxation method is a triangular, or triple-force element, shown in Fig. 6.

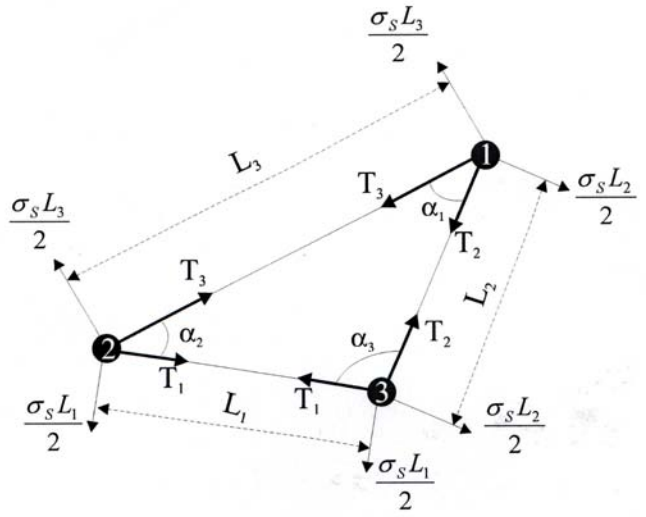

Fig. 6. Triangular, ‘triple-force’ element

The formula: $T_i = \dfrac{\sigma_s L_i}{2\tan\alpha_i}$

represents a transformation of the element surface stress into a discrete set of forces, T_i, acting in the sides of the element. Depending on the value of the enclosed angle α, the element side forces can be either positive, or negative. They are resolved into *x*, *y* and *z* components at the nodes and included directly in the calculation of residual forces within the dynamic relaxation algorithm. However, caution is needed, as cases of ill-conditioning can arise: when the angle α tends to zero, the forces tend to infinity. The problem can be resolved by a sensible discretisation of the surface that ensures ‘healthy’ aspect ratios of the triangles and imposing a limit on α.

4.4.3 Alternative methods of surface discretisation

Alternative types of surface discretisations have been proposed for use with novel, non-finite element approaches [19,20]. The first one[19], which applies to constant tension membranes, makes use of a triangular mesh of points. The resultant forces at the vertices of the triangle are calculated directly from the surface tension, without the need for construction of equivalent plane stress finite elements. These forces are independent of the shape of the triangular mesh. The other type of surface discretisation[20], which also applies to constant tension membranes, but can be adapted to more general cases, makes use of the Laplace-young equation and cubic spline fitting to give a full, piecewise, analytical description of the surface. This approach represents a significant development in surface discretisation, as it produces smooth surfaces with known curvatures that can be used readily to calculate geodesic curves. Geodesics, combined with the knowledge of surface curvatures, facilitate the development of cutting patterns. Also, the spline solution is much closer to the actual surface than a polyhedral surface of elements of the same mesh size[21] .

4.4.4 Mesh control

It is possible to find a shape of a tensioned surface by constraining the x, y movements of the nodes of the initial mesh during form-finding and ensuring equilibrium in z-direction only[16]. This approach was thought to assist with the generation of smooth mesh lines at the end of form-finding so that they could be used for patterning. The idea, however, is fundamentally flawed, because the mesh lines intended to represent seam lines at the patterning stage should correspond to ‘strings’ of constant tension, lying on the surface and following geodesics[15]. These strings need to be in full static equilibrium. Figure 7 illustrates the problem.

(a)

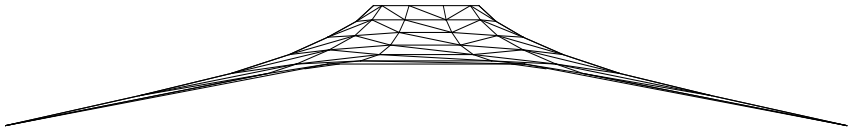

(b)

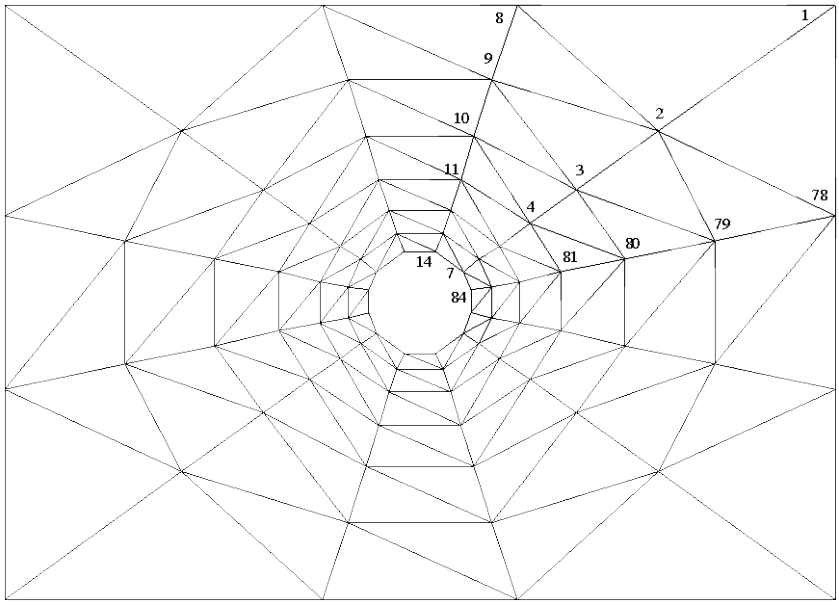

(c)

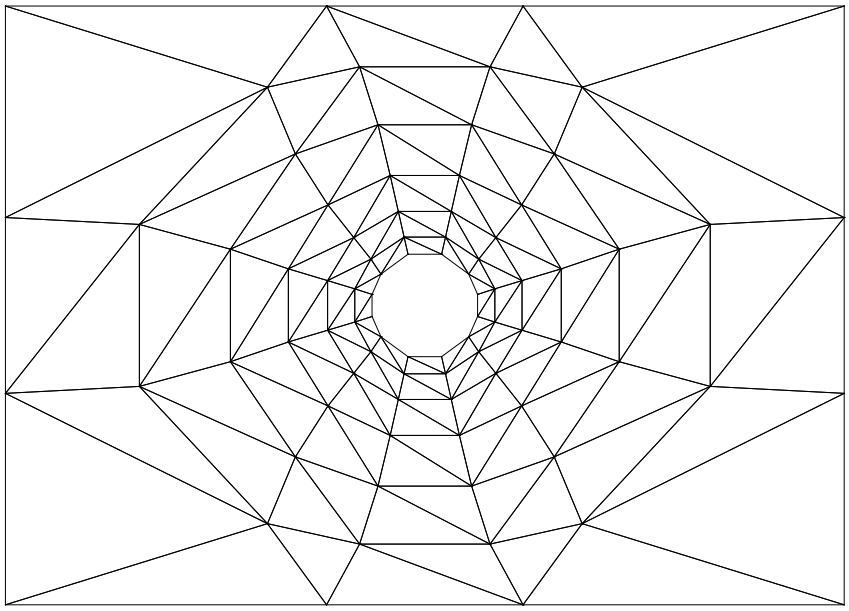

Fig. 7. (a) Elevation of the form-found surface, (b) plan view of the surface obtained with mesh control, (c) plan view of the fully equilibrated surface.

The chosen example is a membrane, which resembles a part of a canopy for the Tête Defence Cube in Paris. The membrane is discretised using triangular elements, as shown. The plan area of the membrane is 5 m by 7 m. The boundaries along the shorter, *x*- dimension are fully fixed, while the two boundaries along the y dimension are fixed only in the *x* and *y* directions. The central boundary, which is circular on plan, has a height of 0.9 m. The membrane has a constant value of prestress, equal to 5 kN/m. The value of the residual force used as a stopping criterion for the iterations was 0.01 kN (a value lower than that showed no significant change in the solution).

The results from form-finding (Fig. 7 (a), (b, and (c) show that mesh control produces the same elevation profile as the unconstrained mesh method. However, the differences lie in the plan views, from which it can be seen that large displacements would have taken place, if the *x*-*y* movements of the nodes were not suppressed. The surface obtained using mesh control is not in full static equilibrium, as shown by the results given in Table 1. They illustrate that very large residual forces still exist in the *x* and *y* directions (several orders of magnitude higher than the prescribed maximum residual force of 0.01 kN) particularly at the nodes along the lines 2-6 and 9-10.

These findings are consistent with the report[22] describing form-finding and patterning of a Papal canopy in Phoenix Park, Dublin. The canopy resembled the membrane shape analysed here, but possessed only one axis of symmetry. Mesh control was applied during form-finding to preserve the radial lines as seam lines in the cutting pattern of the membrane. This led to a very uneven stress distribution in the surface, manifesting itself in wrinkling around the neck of the structure, which required a geometric re-adjustment.

5. Closing remarks

The paper describes three most commonly used computational form-finding methods, which have been implemented in commercial software world wide.

The transient stiffness method exploits load-displacement relationship, which is assumed to be linear throughout. For this to be true, the incremental displacements have to be very small. In the case of an ill-conditioned stiffness matrix, steps need to be taken to remedy the situation, in order to obtain an accurate solution.

The force density method, in its original formulation, is just a tool for generating equilibrated shapes of structures that have the feature of a non-uniform tension field. Additional iterations are required to satisfy the condition of constant tension, as observed in ideal tension structures, such as soap-films. The use of soap-film analogy in form-finding of fabric structures is strongly recommended[15], as it leads to optimal solutions in the form of minimal surface membranes, with a uniform tension field under a permanent load condition, i.e., the pre-tension. This view is reflected in the general recommendation given in the European Design Guide for Tensile Surface Structures[23]. To start, section 8.2 of the Guide contains a somewhat indefinite statement saying that any form-finding method is acceptable, provided it ensures that… "*the resulting surface shape is capable of withstanding the applied loading, while satisfying the constraints imposed by the architectural specification"*… While this appears to give priority to architectural requirements, the statements that follow acknowledge the advantages of using the soap-film analogy. These include: (i) a reduced likelihood of on/off slackening of the fabric under buffeting wind loads, with, consequently, less fatigue of the yarns and their constituent fibres, and (ii) a smaller deformation of the surface due to a change in the warp/weft stress ratio, which is likely to prevent local wrinkling. The Guide also acknowledges the fact that

differentially stressed fabric will creep, over a period of time, towards a form that has a uniform stress distribution.

In the UK, the preferred form-finding method is dynamic relaxation[24]. It is viewed as extremely efficient, robust and accurate. Further, it has an attractive physical interpretation, which aids a good understanding of the solution process.

Acknowledgement. The author wishes to thank her research fellow, J.S. Brew, for supplying Figure 5.

References

1. FORSTER B. Cable and membrane roofs - a historical survey. *Structural Engineering Review*, 1994, **6**, No 3-4, 145-174.

2. ARGYRIS J. H. and SCHARPF D. W. Large deflection analysis of prestressed networks. *Journal ASCE, Structural Division*, ST3, 1972, pp 633-654.

3. ARGYRIS J. H., ANGELOPOULOS T. and BICHAT B. A general method for the shape finding of lightweight tension structures. *Computer Methods in Applied Mechanics and Engineering*, 1974, Vol. 3, pp 135-149.

4. LEONARD J. W. Tension structures. Behaviour and analysis. McGraw Hill Book Company, 1985.

5. MEEK J. L. Computer methods in structural analysis. E&FN Spon, 1991.

6. CHAPRA S. C. and CANALE R. P. Numerical methods for engineers. McGraw Hill, 1985, 2nd edn.

7. WILKINSON J. H. and REINSCH C. Linear algebra. Handbook for automatic computation. Springer, Berlin , 1971.

8. FOX L. An introduction to numerical linear algebra. Clarendon Press, Oxford, 1964.

9. LINKWITZ K. and. SCHECK H. J. Einige bemerkungen zur berechnung von vorgespannten seilnetzkonstruktionen. *Ingenieur - Archiv.* 1971, **40**, 145-158.

10. LINKWITZ K. and SCHECK H. J. A new method of analysis of prestressed cable networks and its use on the roofs of the Olympic Game facilities at Munich IABSE, Amsterdam, 1972.

11. SCHECK H. J. The Force density method for form-finding and computation of general networks. *Computer Methods in Applied Mechanics and Engineering,* 1974, **3**, 115-134.

12. LINKWITZ K. About formfinding of double-curved structures. *Engineering Structures,* 1999, **21**, 709–718.

13. SANCHES J. et al. A multi-step force-density method and surface fitting approach for the preliminary shape design of tensile structures. *Engineering Structures,* 2007, **8**, 1966-1976.

14. GRÜNDIG L. Minimal surfaces for finding forms of structural membranes. *Computers & Structures,* 1988, **30**, 679-683.

15. LEWIS W. J. *Tension structures. Form and behaviour.* Thomas Telford 2003.

16. BARNES M. R. Form and stress engineering of tension structures. *Structural Engineering Review,* 1994, **6**, No. 3-4, 175-202.

17. BREW J. S. and BROTTON D. M. Non-linear structural analysis by dynamic relaxation. *International Journal of Numerical Methods in Engineering,* 1971, **3**, 463-483.

18. LEWIS W. J. The efficiency of numerical methods for the analysis of prestressed nets and pin-jointed frame structures. Computers & Structures, 1989, **33**, no. 3, 791-800.

19. BREW J.S. and LEWIS W.J. Computational form-finding of tension membrane structures - non-finite element approaches: Part 2. Triangular Mesh Discretisation and Control of Mesh Distortion in Modelling Minimal Surface Membranes. *International Journal for Numerical Methods in Engineering,* 2003, **56**, 669-684.

20. BREW J.S. and LEWIS W.J. Computational form-finding of tension membrane structures - non-finite element approaches: Part 1. Use of cubic splines in finding minimal surface membranes. *International Journal for Numerical Methods in Engineering,* 2003, **56**, 651-668.

21. BREW J.S. and LEWIS W.J. Computational form-finding of tension membrane structures - non-finite element approaches: Part 3. Comparison of mesh constraint methods. *International Journal for Numerical Methods in Engineering,* 2003, **56**, 685-697.

22. DAY A. Form-finding, Control and modification for tension structures. *The Arup Journal,* 1980, 19-20.

23. FORSTER B. and MOLLAERT M. *European design guide for surface tensile structures.* Tensinet 2004.

24. WAKEFIELD D. S. Engineering analysis of tension structures: theory and practice. *Engineering Structures,* 1999, **21**, no. 8, 680-690.